A comparative study of Al and LiF:Al interfaces with Poly (3-Hexylthiophene) using bias dependent photoluminescence technique.

Vipul Singh[a,*], Anil K Thakur[a], Shyam S Pandey[a], Wataru Takashima[b], and Keiichi Kaneto[a]

[a] *Department of Biological Functions and Engineering, Graduate School of Life Sciences and Systems Engineering, Kyushu Institute of Technology, 2-4 Hibikino, Wakamatsu, Kitakyushu, Fukuoka 808-0196, Japan.*

[b] *Research Center for Advanced Eco-fitting Technology, Kyushu Institute of Technology, 2-4 Hibikino, Wakamatsu, Kitakyushu, Fukuoka 808-0196, Japan.*

[*]Email: vipul.lsse@gmail.com

Abstract

The qualitative nature of the interface of poly (3-hexylthiophene) (P3HT) with Aluminum (Al) and LiF modified Aluminum (LiF:Al) has been studied using photoluminescence (PL) spectra. It was observed that coating Al on pristine P3HT film resulted in an increase in the degree of intrachain disorder. Also, a blue shift in the peak PL intensity was observed. These observations have been explained on the basis of intrachain disorder induced by the deposition of Al via thermal evaporation on P3HT film. Furthermore, bias dependence of PL spectra for ITO/P3HT/Al and ITO/P3HT/LiF:Al type Schottky cells was studied. Under the reverse bias conditions, PL quenching was found to relate directly to the depletion layer width. The increase in depletion width was found to be higher in the Al cell as compared to that of the LiF:Al

cell. However, the photocurrents were higher in LiF:Al coated cells. These observed results have been explained on the basis of the difference in their respective band alignment.

Keywords: interface, photoluminescence, intrachain excitons, depletion layer, poly (3-hexylthiophene), LiF, photocurrent.

1. Introduction

In the recent past π conjugated polymer based electronic devices viz. polymeric solar cells (PSCs) [1, 2], polymeric light emitting diodes (PLEDs) [3, 4] and polymeric field effect transistors (PFETs) [5] have gained special interest due to their excellent transport properties as well as their potential application for the development of cheap and flexible electronic devices [6, 7]. It has been observed that the interface between various polymeric layers and also between polymer and metal is very crucial for the high performance and development of these devices [8, 9]. Treatment of bare SiO_2 surface by a silanizing agent like 1,1,1,3,3,3- Hexamethyldisilazane (HMDS) is one such example of the significant role played by the nature of interface in governing the functionality of these devices [10, 11].There are various techniques to study the interface of any two given dissimilar materials viz. Ultraviolet photoelectron spectroscopy (UPS), Photoluminescence (PL), X-ray Diffraction (XRD) etc.

PL emission spectrum refers to the spontaneous emission of light from a material under optical excitation and could be used to characterize a variety of material parameters. Features of PL spectra can be used to identify surfaces, interfaces, impurity

levels and interface roughness [12, 13]. On one hand, the transient PL intensity yields the lifetime of non-equilibrium interface and bulk states, while on the other hand PL intensity variation under an applied field gives an estimate of the built in field near the interface. In addition, thermally activated processes can also cause changes in PL intensity. A bias dependent PL can be used to study the different competing mechanisms of exciton generation, diffusion and dissociation [14, 15]. Thus a bias dependent PL spectrum is of critical importance as it gives information regarding the electro-luminescence (EL), photoconduction and photovoltaic effects. EL efficiency is a determining factor for the performance of PLEDs and is directly related to PL efficiency [16], as both originate from the same intermediate state, i.e. excitons [17].

LiF:Al electrodes are widely used for the enhancement of the efficiency of PLEDs and PSCs. However, the underlying mechanisms are still under investigation. Several mechanisms have been suggested thus far [18-22], including (i) the lowering of work function of Aluminum; (ii) Dissociation of LiF and subsequent chemical reaction (doping) of the organic semiconductor; (iii) Formation of a dipole layer leading to a vacuum level offset between the organic layer and the Al; and (iv) protection of the organic layer from the hot Al atoms during thermal deposition. Despite of these proposed mechanisms the exact role of LiF is not yet completely understood. Although a good deal of efforts have been devoted to clearly explain the role of LiF in the efficiency enhancement of PLEDs, but the underlying mechanisms for the PSCs efficiency improvement by LiF inclusion has not yet been discussed in much detail.

In this article, we report the effect of coating Al on to P3HT. The blue shift in the peak energy and a relative increase in the shoulder peak at higher energy in PL emission

have been explained on the basis of increase in the degree of intrachain disorder, resulting in a relatively higher population of intrachain excitons. We further report the different types of PL quenching pattern obtained for the two types of schottky cells fabricated with and without a thin layer of LiF. The difference has been explained on the basis of the nature of interface of P3HT with Al alone and that of Al in the presence of a thin layer of LiF.

2. Experiment

Six different types of samples namely A, B, C, D, E and F, have been fabricated as shown in Fig. 1 (a, b, c, d, e & f) for the purpose of PL measurements. Prior to sample fabrication, glass substrates (for samples A, B, C and D) and ITO coated glass substrates (for samples E and F) were cleaned using NH_3 and H_2O_2 followed by sonication in chloroform and iso propanol solution. Samples A and B were spin coated at {1500 (30s), 3000 (10s)} rpm with a thin film of regioregular (rr) P3HT (Merck Lisicon SP001, having a average Molecular weight of 44000, and 96% regioregularity) from its chloroform solution on to the cleaned glass substrate, followed by annealing at $100^0 C$ (under vacuum for 2 hours). Samples A were divided into two lots. First lot was coated with 2.5 nm Al (under vacuum, $P = 2.0 \times 10^{-6} Torr$). The second lot was coated with 1 nm LiF prior to coating 2.5 nm Al under identical conditions. Similarly Sample B was divided into two lots, first lot was coated with 30 nm Al while the second lot was coated with 1 nm LiF followed by 30 nm Al. Sample C was divided into three lots, while first lot was spin coated with regioregular (rr) P3HT (as obtained from Merck) at {1500 (30s), 3000 (10s)} rpm, the second lot was spin coated with non-regio controlled (nrc)

P3HT (synthesized, using $FeCl_3$ method, having a regioregularity of 88%) at {1500 (30s), 3000 (10s)} rpm [38,39] and the third lot was spin coated at {1500 (30s), 3000 (10s)} rpm with regiorandom (rrnd) P3HT (used as obtained from Aldrich, having 1:1 HT:HH coupling). While sample C was half coated 30 nm thick Al on to the top of the film, However, sample D was coated with 30 nm thick Al prior to spin coating at {1500 (30s), 3000 (10s)}rpm the rr P3HT film, as is also clear from Fig. 1 (c & d). On one hand all the lots of Sample C were used to study the effect of intrachain disorder on the absorption and emission spectra. The first lot of Sample C coated with rr P3HT was also used to compare with Sample D for the effect of coating Al on top and bottom of the film as will be discussed in detail in the next section. Figure 1(e & f) show the schematic diagram of the sample fabricated for the bias dependent PL spectra of the schottky cell. It should be noted that the Cells E and F were fabricated in ITO/P3HT/Al and ITO/P3HT/LiF:Al type device configurations, as is also shown in Fig. 1(e & f) respectively. Both LiF and Al were deposited by thermal evaporation. For the fabrication of ITO based sandwich cells, ITO coated glass substrates were patterned by etching in dilute HCl solution with Zinc powder to fabricate the ITO bottom electrodes, which were subsequently spin coated at {1500 (30s), 3000 (10s)}rpm with chloroform solution of rr P3HT. The Thickness of these films was later determined to be 200 nm. All the film Thicknesses were measured using Dektak Surface Profiler. Thicknesses of sample A and B were determined to be 79 and 55 nm respectively, while both samples C and D were of identical thickness of 60 nm.

PL measurement was done under ambient conditions using photonic multi channel analyzer, (Hamamatsu PMA-11), kept at a distance of 70 cm from the sample. A He-Cd

Laser (300 mW, CW, 442 nm, Kimmon IK4121R) was used as a light-pumping source. The intensity of photons incident on the sample was later calculated to be 0.15 W/cm^2 incident at an inclination of about 30^o to the normal. In-situ electrical bias was applied on the cells using Keithley 6517 A electrometer. ITO was biased as an cathode under the reverse bias direction, as is shown in Fig. 2(a). Care was also taken to avoid over exposure of the sample to the laser beam. It should also be noted that all the samples except sample D were illuminated from the glass side. However, Sample D was illuminated from the film side. The details of which will be discussed in the next section.

3. Results and discussion

Figure 3 shows the effect of an island deposition of LiF (1 nm) and LiF (1 nm) followed by Al (2.5 nm) on rr-P3HT film. It was observed that coating LiF and Al both separately onto a P3HT film results in the quenching of the PL signal [24]. The PL emission intensity I_{PL} is given by

$$I_{PL} = \eta_{PL}\eta_C I_{abs} \qquad \text{Eq (1)}$$

Where η_{PL}, η_C and I_{abs} denote the PL efficiency [25, 26, 40], efficiency of the detector and the intensity of the light absorbed, respectively. It should be noted that η_{PL} itself is given by the relation under the similar assumptions as in [26, 40].

$$\eta_{PL} = \left(\frac{K_R}{K_R + K_{NR}} \right) \qquad \text{Eq (2)}$$

Where K_R and K_{NR} denote the radiative and non radiative decay rate constants of excitons. The observed effects in Fig. 3 can be explained on the basis of the fact that deposition of a small amount of external species leads to an increase in the non radiative

decay paths near the interface, which then leads to decrease in the PL efficiency resulting in the observed PL quenching. Our previous report [24] also indicates that the PL quenching was observed by coating the Al and LiF over layers on a P3HT film separately. Although the extent of PL quenching was different in the two cases. It was observed that coating LiF leads to increase in the K_{NR} while coating Al leads to PL quenching due to dissociation of excitons near the Al/P3HT interface due to high built in field of the depletion layer. Similarly Fig. 3 shows that increasing the population of the impurities i.e. coating LiF (1 nm) and then further coating Al (2.5 nm) resulted in increasing level of PL quenching. However, when the thickness of Al was increased from 2.5 nm to 30 nm the PL intensity increased as can be seen in Fig. 4. This effect has been observed due to double excitation of the film by the incident laser beam due to a strong reflection occurring from the top coated Al layer [26]. It is important to note that unlike Fig. 3, In Fig. 4 the PL counts for P3HT/LiF:Al samples were higher than that of P3HT/Al samples. Figure 4 also shows an increase in the high energy shoulder peak occurring due to the Al coating on to the top of pristine P3HT film. Another significant point is the blue shift shown by the peak PL emission (E = 1.702 eV) spectra due to Al coating.

In order to ascertain the exact origin of this behavior another experiment was performed in which both top and bottom Al coated samples, namely samples C and D were fabricated. While sample C was illuminated by laser light from the glass facing side contrary to the sample D which was illuminated from the film facing side. This was done primarily because the bottom Al layer (sample D) would screen the intensity of the laser excitation light and would also largely block the PL emissions from the underlying P3HT

bulk layer, if illuminated from the glass side. It is a general observation that intensity of PL signal is also correlated with the degree of roughness near the interface. As can be clearly seen from Fig. 5, the PL counts for pristine P3HT film was higher in the case of sample C compared to that of sample D. It should be noted that both sample C and D showed an increase in the PL intensity, a clear cut evidence of dual excitation of the bulk in the two cases. However, unlike sample C, Sample D did not show any increase in the high energy shoulder peak, clearly indicating that such an effect is taking place due to the thermal deposition of Al over the pristine P3HT films. The results were similar to the one observed by Thakur et al. [37], although in their case they studied the effect of coating gold (Au) on Pristine P3HT film. In another similar report Brown et al. [30] also observed that the high energy peak in the PL emission occurs due to the intrachain excitons [34] and that the intrachain excitons are highly affected by the intrachain disorder contrary to the interchain excitons. Thus it can be concluded that coating Al on to the top of a film results in an increase in the intrachain disorder due to the thermal energy transfer from the hot Al atoms coated on P3HT film during the thermal evaporation process. It is known that the spin coated P3HT films are composed of microcrystalline domains embedded in an amorphous matrix. Inside these domains the polymers π-stack in one direction and form lamella of interlocking chains in the other direction. Usually the side alkyl chains try to orient themselves in a least strained position (energetically). Although this type of rearrangement is less pronounced in spin coated P3HT films as compared to dip coated or casted P3HT films [34-36]. However, as a result of this energy transfer between Al and immediate P3HT, polymer chains tend to have a more strained structure of the hexyl group attached to the polymer backbone,

resulting in an increase in the intrachain disorder. Also, since some of these chains may be part of a micro crystalline domain, thus an intrachain disorder may result in a decrease of degree of π-stacking of these microcrystalline domains and hence of the films at the macro level, resulting in the blue shift of the PL emission peak occurring at 1.702 eV, as shown in Fig. 4. However, the absence of any such blue shift in Fig. 3 in which island deposition of Al and LiF:Al was done is probably due to the fact that the thickness of Al and LiF in these cases were too less to result in any observable changes.

In order to have detailed insight about the intrachain disorder effects on PL, we further fabricated three types of films, first was coated with rr-P3HT, the second one was coated with non-regio controlled (nrc) P3HT and the third with rrnd P3HT (as obtained from Aldrich). The normalized absorption and emission spectra of these films have been shown in Fig. 6. It is clearly evident from this figure that the $\pi - \pi^*$ transition band of the films was blue shifted [31] in the increasing order of their regio randomness, suggesting that higher degree of regioregularity leads to decrease in the band gap. This effect is attributed to the lesser degree of π conjugation on the parent chain in rrnd P3HT. Even the Band edge appears to be blue shifted in the increasing order of regio randomness of these P3HT films. Another striking feature is that the absorption of rr P3HT has three distinct peaks occurring at (E = 2.13, 2.33 and 2.50 eV) respectively. Pandey et al. [31] have demonstrated that the lowest energy peak in the absorption spectra (at 2.13 eV) corresponds to 0-0 transition and is related to the conformational order in the chains, while the peak at 2.33 eV corresponds to 0-1 transition and is related to the interchain ordering or the π stacking of the various chains. While the main peak near 2.50 eV corresponds to the 0-2 transition. Compared to the rr-P3HT these peaks

were less pronounced in nrc P3HT and nearly vanished in rrnd P3HT film. It should also be noted that a clear blue shift in the absorption spectra was obtained for rrnd P3HT. However, only a little blue shift was obtained in nrc P3HT. This is probably due to high degree of regio regularity in these samples despite of being synthesized by $FeCl_3$ method.

Further if we look at the PL emission spectra of these films, we find that there is almost no shift in the emission spectra of rr-P3HT and nrc P3HT, on the contrary a large blue shift is obtained in the emission spectra of rrnd P3HT as compared to that of rr-P3HT. Further it must be noted that the 0-0, 0-1 and 0-2 transitions for the emission spectra of rr-P3HT and nrc P3HT occur at E = 1.89, 1.7 and 1.5 eV, respectively. However, the corresponding 0-0, 0-1 and 0-2 transitions for rrnd P3HT occur at E = 2.07, 1.98 and 1.74 eV respectively. As can also be seen from Fig. 6 that the intensity of shoulder peaks at 1.5 eV and 1.89 eV increase in the case of nrc P3HT compared to the rr- P3HT. Brown et al. [30] have emphasized that the high energy peak at E = 1.89 eV is highly affected by the intrachain disorder, i.e. the degree of regioregularity of the polymer. Thus, the relative increase of the high energy peak as can be seen from the normalized PL spectra of the two films from Fig. 6 is owing to the lower degree of regio regularity on a single polymer chain in nrc P3HT. However, Brown et al. also pointed out that the peak in the emission spectra corresponding to interchain excitons (at E = 1.702 eV) doesn't get affected by the local order that is the regioregularity, as clearly corroborated by the Fig. 6. In the case of rrnd P3HT the highest energy peak at E = 2.07 eV corresponding to 0-0 transition has relatively higher intensity as compared to the 0-1 transition at E = 1.98 eV. This is because the intrachain disorder is highest in rrnd P3HT and hence the 0-0 transition in rrnd P3HT has a higher intensity as compared to 0-1

transition. Kaneto et al. [32] presented the PL spectra of an electrochemically synthesized polymer, which showed very low contributions from the interchain emissive state. At the same time it must be noted that the emission at E = 1.5 eV is also relatively increased in the case of nrc P3HT. This peak relates to the conformational order and as we know that the conformational order decreases in the nrc P3HT film resulting in relatively higher values of observed PL intensity (at E = 1.5 eV). In another interesting work Tanaka et al. [34] have demonstrated a clear cut change in the characteristic PL emission spectra by the fine control of the blending ratios of rr and rrnd P3HT.

In order to clearly understand the difference in the nature of interface we fabricated two types of cells E and F, for the purpose of study of the bias dependence photoluminescence quenching in the two cells. Figure 2(b) shows the effect of increasing reverse bias voltage results in increasing the depletion layer thickness from w_0 (at 0 V) to $w(V)$ at any reverse bias voltage V and hence resulting in PL quenching due to lessening of the thickness of active P3HT layer. It should be noted that although the depletion width at zero bias for cell E $(w_0)_E$, has been found to be slightly less than the depletion width at zero bias for cell F $(w_0)_F$ the higher value of PL counts in cell E is primarily due to the significant difference in the value of the parameter χ as has been defined in ref [26]. Although at present the exact origin of this behavior is not completely understood.

PL quenching Q_{PL} [26-28, 40] as defined by eq (3)

$$Q_{PL} = \left(I_{PL}(0) - I_{PL}(V)\right)/I_{PL}(0) \qquad \text{Eq (3)}$$

Where $I_{PL}(0)$ and $I_{PL}(V)$ denote the PL intensity at zero bias and at a bias V respectively. Figure 7 shows the quenching pattern for cell E and F and exhibits that a

relatively higher level of quenching was observed in cell E as compared to that in cell F with the increasing reverse bias voltage. Similar results have been observed by Markov et al also. Although there are reports of PL quenching due to injected charge carriers [40-42] but such an effect is negligible in the present case as our discussion here concerns only with the reverse bias regime. Therefore, from Eq. (3) it is clear that the quenching directly relates to the amount of light absorbed by the bulk of semiconductor. Using the similar analysis as was given in ref [26], the depletion width dependence of bias voltage was plotted for cells E and F using the bias dependence of quenching of these cells. The change in the depletion width $\delta w(V)$ has been found to be related to Q_{PL} as is given by eq (4),

$$\delta w(V) = \frac{1}{\alpha} \ln \left| \frac{\sqrt{(A+2B)^2 + 4BQ_{PL}} - A}{2B} \right| \qquad \text{Eq (4)}$$

Where the constants A and B were determined as described in ref [26, 40]. The plot of $\delta w(V)$ against the applied bias V for the two cells has been shown in the Fig. 8. The change in the depletion width as a function of voltage was found to be more prominent in the cell E as compared to cell F. Thus it can be concluded that the presence of LiF near the interface limits the extent of modulation of the depletion layer with the applied reverse bias voltage. Figure 8 shows a clear cut deviation of the depletion width from eq (5) [26, 29], that itself has been derived assuming a uniform charge carrier density. However, in a polymeric semiconductor like P3HT the charge carrier density is non uniform, thus resulting in the observed deviation. Takshi et al. also demonstrated similar observations in ref [29].

$$w = \sqrt{2\varepsilon_s (V_{bi} - V)/qN_A} \qquad \text{Eq (5)}$$

Where w denotes the depletion layer width. ε_s, q, V_{bi}, N_A denote the dielectric permittivity , charge of an electron, built in potential and Acceptor charge density respectively. Figure 9 on the other hand shows higher level of photocurrents in cell F as compared to that for the cell E. The photocurrents are found to increase with the increasing application of reverse bias voltage for the two cells. Here, it must be noted that the improvement in the PLEDs is mainly due to the improved injection of the electrons from the cathode into the LUMO of n-type semiconductor. However in our study only p-type material i.e. P3HT was used, and the IV characteristics reflect the hole transport. The holes are injected from ITO into the HOMO of P3HT and from there into the Fermi level of Al. Thus, a decrease in the forward bias current was observed for cell F as is shown in inset of Fig. 9, although the built in voltage V_{bi} was found to increase upon the LiF coating.

Brabec et al [21] studied the effect of LiF in Bulk hetero junction solar cells. It was observed that including a thin layer of LiF improved the solar cell efficiency of the PSCs considerably. However, in their final conclusion they attributed this effect to either the orientation of LiF or chemical reactions leading to charge transfer across the interface, thus resulting in the formation of dipole moment across the junction. However, the absence of memory currents in LiF coated photo induced memory devices [24] clearly rules out any such possibility. Thus, we conclude that it is the orientation of LiF near the interface that results in the dipole moment across the junction. At the same time it is this dipole moment of LiF that leads to high localized field as is shown by the offset level Δ in the band diagram in Fig. 10. The lesser values of depletion width of the cell F probably resulted due to the less steep band bending of P3HT in cell F as is shown in the

Fig. 10. However, the high localized field near the interface in cell F resulted in higher values of photocurrents, as photocurrents are generated by the field assisted dissociation of excitons. A highly localized Field near the interface ensures effective dissociation of excitons. Thus we conclude that it is the dipole moment of the LiF molecule itself that leads to a highly localized field, resulting in the improvement of the Solar cell efficiency.

4. Conclusion

Finally we would like to conclude two main points. First is that the Al coating on to the top of polymer pristine film has identical effects as that observed by decreasing regio regularity of the polymer chain. Both of these effects actually originate from the intrachain excitons which are highly dependent on the local order on a chain. The second point is that the depletion layer is less modulated in cell F compared to cell E. Although an overall high Electric field is developed near the interface in cell F. Inclusion of LiF improves the solar cell efficiency of PSCs due to the fact that LiF is a strong ionic molecule having high dielectric constant, which results in a strong localized electric field due to the dipole formation by these molecules, further resulting in the observed lower values of depletion layer and higher values of the photocurrents in LiF:Al modified cathode type Schottky devices.

Acknowledgements

This work was supported by Grant in Aid for Science and Research in priority area "Super hierarchical structures" from Ministry of education, culture, sports, science and

technology, Japan. One of the authors (V.S.) would further like to thank Heiwa Nakajima Foundation for providing the scholarship.

References

[1] H. Spanggaard and F. C. Kerbs, 2004 Sol. Energy. Mat. Sol. Cells. 83 (2004) 125.

[2] Y. Kim, S. A. Choulis, J. Nelson, D. D. C. Bradley, S. Cook S and J. R. Durrant, J Mat. Sci. 40 (2005) 1371.

[3] T. F. Guo and Y. Yang, Appl. Phys. Lett. 80 (2002) 148.

[4] P. Pneumans, A. Yakimov and S. R. Forrest, J. Appl. Phys. 93 (2003) 3693.

[5] V. Singh, M. Yano, W. Takashima and K. Kaneto, Jpn. J. Appl. Phys. 45 No. 1B (2006) 534.

[6] D. A. Bernards, T. Biegala, Z. A. Samuels, J. D. Slinker, G. G. Malliaras, S. F. Torres, H. D. Abruna and J. A. Rogers, Appl. Phys. Lett. 84 (2004) 3675.

[7] T. W. Lee, S. Jeon, J. Maria, J. Zaumseil, J. W. P. Hsu and J. A. Rogers, Adv. Func. Mat. 15 (2005) 1435.

[8] J. C. Scott, J. Vac. Sci. Tech. A 21 (2003) 521.

[9] W. R. Siliveira and J. A. Marohn, Phys. Rev. Lett. 93 (2003) 116104.

[10] S. Grecu, M. R. Buck, A. Opitz and W. Brutting, Org. Elec. 7 (2006) 276.

[11] T. P. I. Saragi, T. F. Lieker and J. Salbeck, Synth. Met. 148 (2005) 267.

[12] B. Deveaud, A. Regreny, J. Y. Emery and A. Chomette, J. Appl. Phys. 59 (1986) 1633.

[13] B. S. Elmann, E. S. Koteles, C. Jagannath, Y. J. Chen, S. Charbonneau and M. L. W. Thewalt, Proc. SPIE 794 (1987) 44.

[14] R. Kersting, U. Lemmer, M. Deussen, H. J. Bekker, R. F. Mahrt, H. Kurz, V. I. Arkhipov, H. Bassler and E. O. Gobel, Phys. Rev. Lett. 73 (1994) 1440.

[15] G. Yu, J. Gao, J. C. Hummelen, F. Wudl and A. J. Heeger, Science 270 (1995) 1789.

[16] M. Segal, M. A. Baldo, R. J. Holmes, S. R. Forrest and Z. G. Soos, Phys. Rev. B. 68 (2003) 075211.

[17] N. S. Sariciftci, L. Smilowitz, A. J. Heeger and F. Wudl, Science 258 (1992) 1474.

[18] Y. D. Jin, X. B. Ding, J. Reynaert, V. I. Arkhipov, G. Borghs, P. L. Heremans and M. Van der Auweraer, Org. Elec. 5 (2004) 271.

[19] T. Yokoyama, H. Ishii and Y. Ouchi, Surf. Rev. Lett. 9 No. 1 (2002) 425.

[20] M. A. Baldo and S. R. Forrest, Phys. Rev. B. 64 (2001) 085201.

[21] C. J. Brabec, S. E. Shaheen, C. Winder, N. S. Sariciftci and P. Denk, Appl. Phys. Lett. 80 No. 7 (2002) 1288.

[22] S. Sohn, K. Park, D. Lee, D. Jung, H. M. Kim, U. Manna, J. Yi, J. Boo, H. Chae and H. Kim, Jpn. J. Appl. Phys. 45 No. 4B (2006) 3733.

[23] D. E. Markov and P. W. M. Blom, Phys. Rev. B. 72 (2005) 161401.

[24] V.Singh, A. K. Thakur, S. S. Pandey, W. Takashima and K. Kaneto, Jpn. J. Appl. Phys. 47 No. 2B (2008) 1251.

[25] H. Becker, S. E. Burns and R. H. Friend, Phys. Rev. B. 56 (1997) 1893.

[26] V. Singh, A. K. Thakur, S. S. Pandey, W. Takashima and K. Kaneto, Appl. Phys. Exp. 1 (2008) 021801.

[27] S. Tasch, G. Kranzelbinder, G. Leising and U. Scherf, Phys. Rev. B. 55 No. 8 (1997) 5079.

[28] M. C. J. M. Vissenberg and M. J. M. de Jong, Phys. Rev. B. 57 (1998) 2667.

[29] A. Takshi, A. Dimopoulos and J. D. Madden, Appl. Phys. Lett. 91 (2007) 083513.

[30] P. J. Brown, D. S. Thoma, A. Kohler, J. S. Wilson, J. S. Kim J S, C. M. Ramsdale, H. Sirringhaus and R. H. Friend, Phys. Rev. B. 67 (2003) 064203.

[31] S. S. Pandey, W. Takashima, S. Nagamatsu, T. Endo, M. Rikukawa and K. Kaneto, Jpn. J. Appl. Phys. 39 (2000) L94.

[32] K. Kaneto, Y. Kohno and K. Yoshino, Solid State Commun. 51 (1984) 267.

[33] R. Hidayat, A. Fuji, M. Ozaki and K. Yoshino, Jpn. J. Appl. Phys. 40 (2001) 7103.

[34] H. Tanaka, Y. Yoshida, T. Nakao, N. Tsujimoto, A. Fujii and M. Ozaki, Jpn. J. Appl. Phys. 40 (2006) L1077.

[35] W. Takashima, S. S. Pandey, T. Endo, M. Rikukawa, N. Tanigaki, Y. Yoshida, K. Yase and K. Kaneto, Thin Solid Films 393 (2001) 334.

[36] G. Wang, T. Hirasa, D. Moses and A. J. Heeger, Synth. Met. 146 (2004) 127.

[37] A. K. Thakur, A. K. Mukherjee, D. M. G. Preethichandra, W. Takashima and K. Kaneto, J. Appl. Phys. 101 (2007) 104508.

[38] S. S. Pandey, W. Takashima, S. Nagamatsu, T. Endo, M. Rikukawa and K. Kaneto, Jpn. J. Appl. Phys. 39 (2000) L94.

[39] M. R. Anderson, D. Selse, M. Berggeren, H. Jarvinen, T. Hjertberg, O. Inganas, O. Wennerstrom and J. E. Osterholm, Macromolecules 27 (1994) 6503.

[40] V. Singh, A. K. Thakur, S. S. Pandey, W. Takashima and K. Kaneto, Synth. Met. doi:10.1016/j.synthmet.2008.01.013 .

[41] Y. Luo, H. Aziz, G. Xu and Z. D. Popovic, Chem. Mater. 19 (2007) 2288.

[42] H. S. Majumdar, C. Botta, A. Bolognesi, A. J. Pal, Synth. Met. 148 (2005) 175.

Figure Captions

Fig. 1 Shows the Schematic diagram of (a) (Sample A) Island deposition of LiF (1 nm) followed by Al (2.5 nm) on a P3HT coated glass substrate (b) (Sample B) Island deposition of LiF (1 nm) followed by Al (30 nm) on a P3HT coated glass substrate (c) (Sample C) Half coated with Al (30 nm) on the top (the hashed portion shows the depletion layer formed at the Al/P3HT interface) (d) (Sample D) Half coated with Bottom Al (30 nm) electrode (e) (Sample E) a diode cell having ITO/P3HT/Al configuration (f) (Sample F) a diode cell having ITO/P3HT/LiF:Al configuration.

Fig. 2 (a) Shows the typical biasing arrangement under the reverse bias conditions (b) Shows the effect of increasing reverse bias on the depletion layer width leading to PL quenching.

Fig. 3 PL Quenching effect due to island deposition of Al and LiF:Al on pristine P3HT film.

Fig. 4 The effect of coating 30 nm thick Al on pristine and LiF (1 nm) coated P3HT films on the PL of P3HT.

Fig. 5 Effect of top and bottom coating of Al (30 nm) on the PL spectra of P3HT films taken from glass side (glass facing) or from film side (film facing).

Fig. 6 Normalized absorption and emission spectra of rr P3HT, nrc P3HT and rrnd P3HT films.

Fig. 7 Plot of PL quenching Q_{PL} versus the reverse bias voltages V for cell E and F.

Fig. 8 Change in depletion width δw as a function of voltage for cell E and F.

Fig. 9 Photocurrents as a function of reverse bias voltages for cell E and F. Inset shows the forward bias currents for cell E and F.

Fig. 10 Band diagram for the cell E and F at zero bias condition.

Figure 1

Click here to download high resolution image

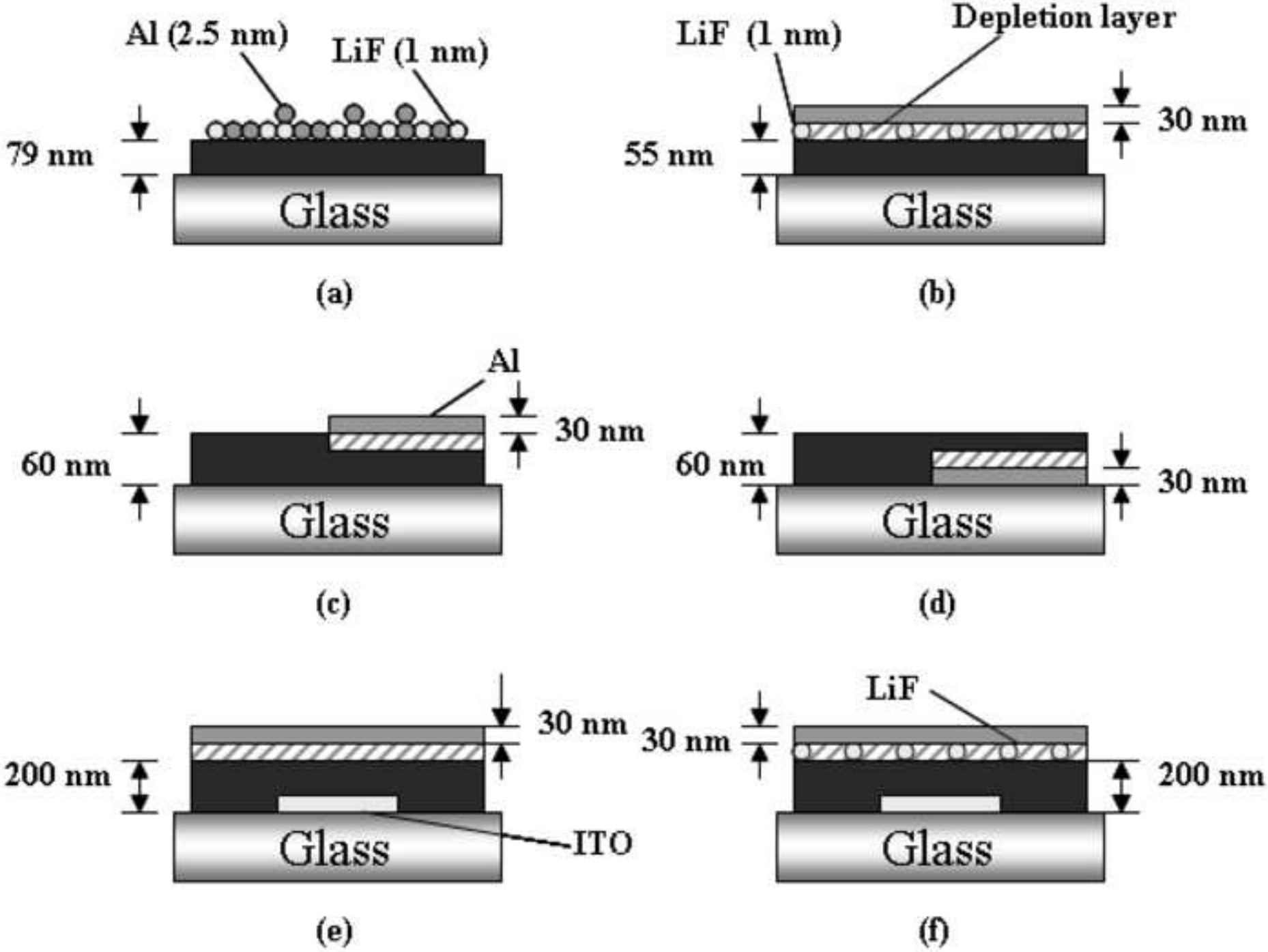

Figure 2
Click here to download high resolution image

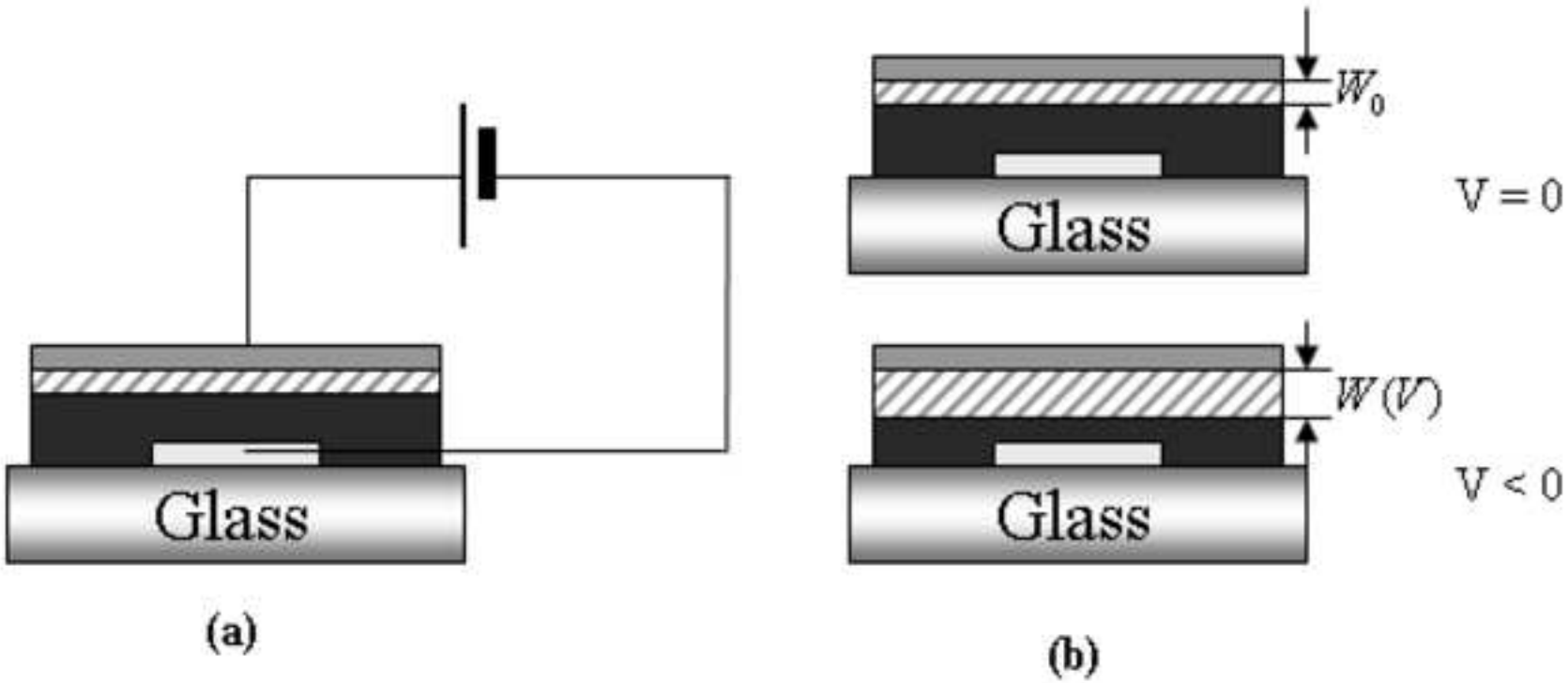

Figure 3

Click here to download high resolution image

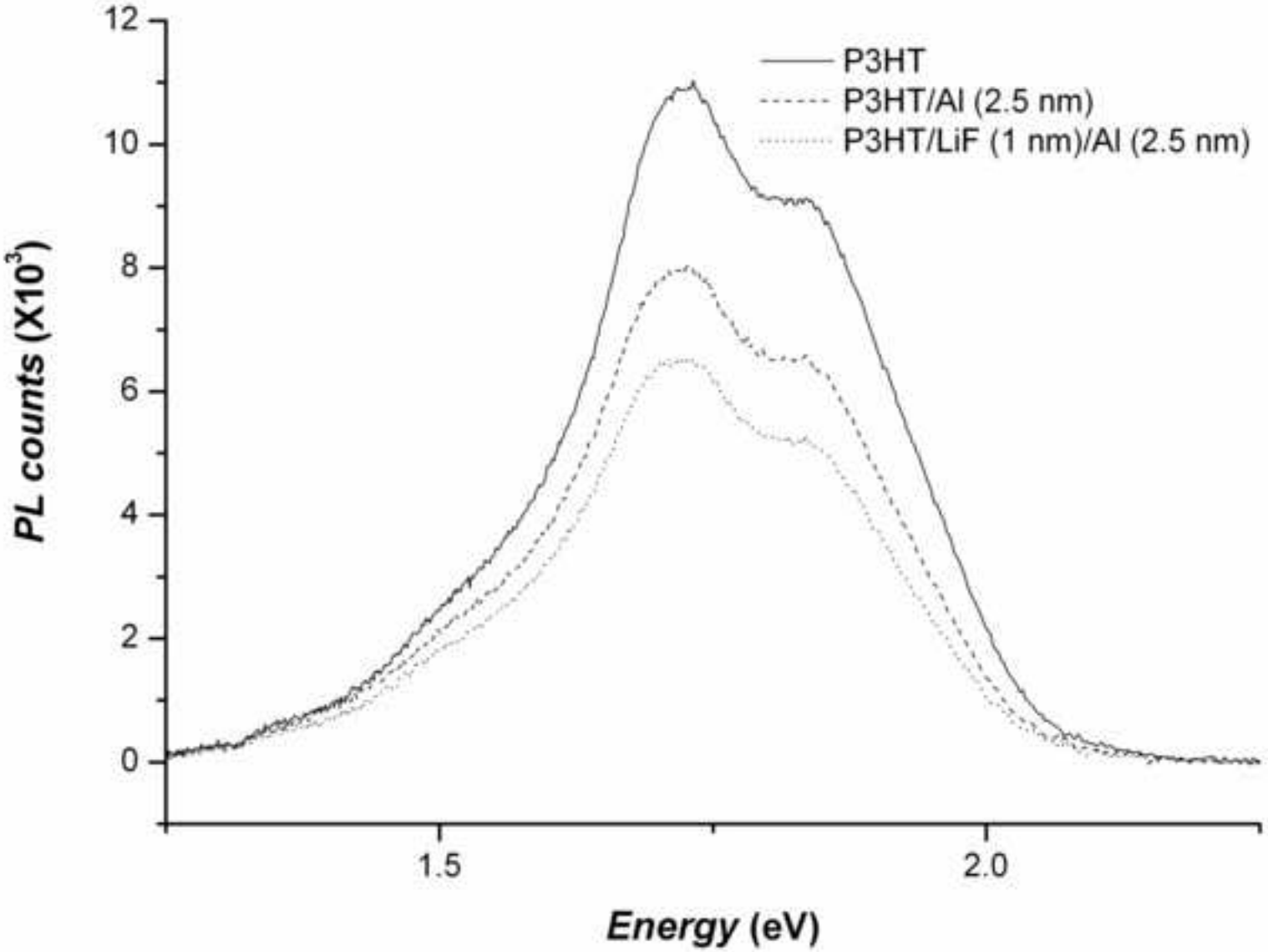

Figure 4

Click here to download high resolution image

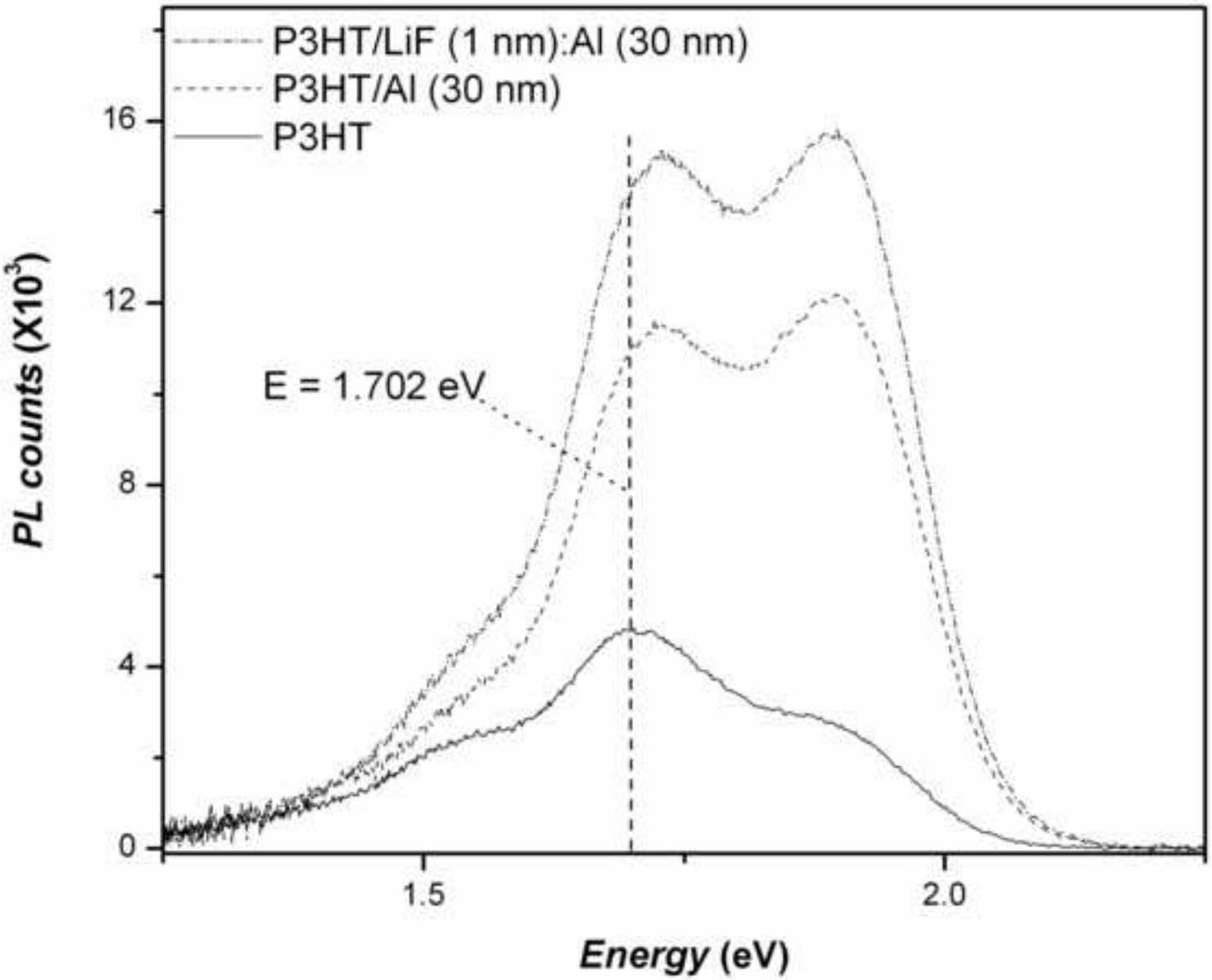

Figure 5

Click here to download high resolution image

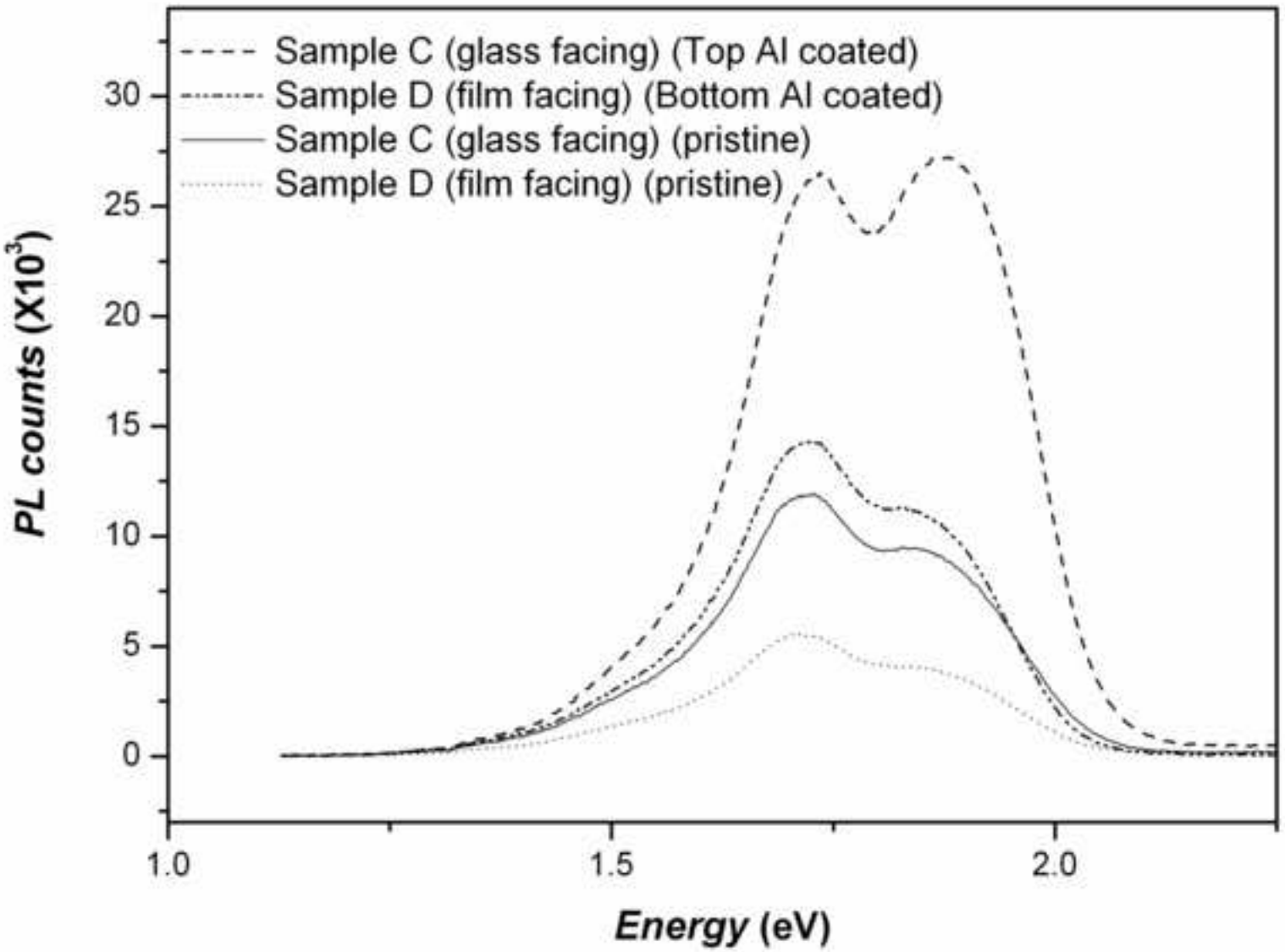

Figure 6
Click here to download high resolution image

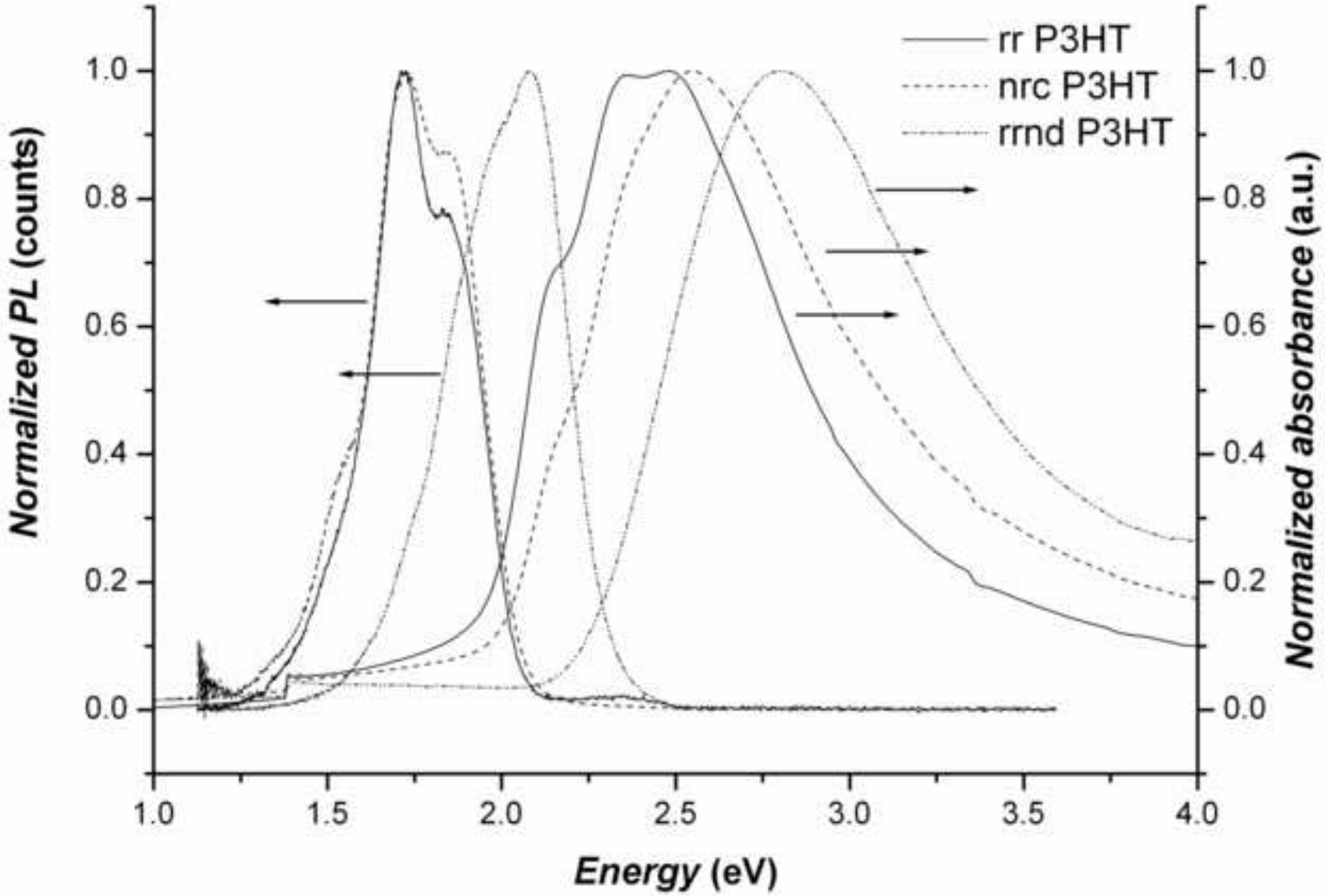

Figure 7

Click here to download high resolution image

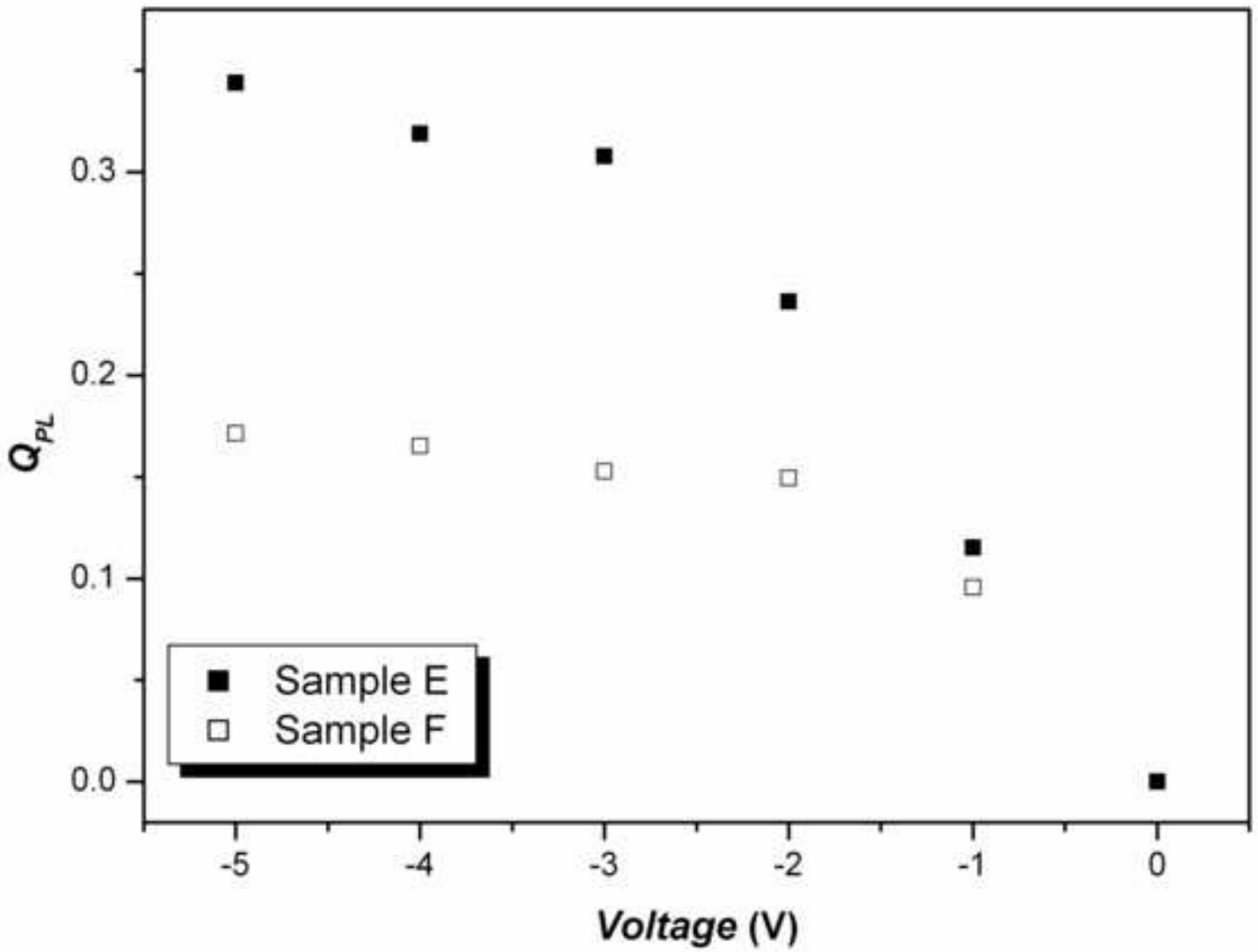

Figure 8

Click here to download high resolution image

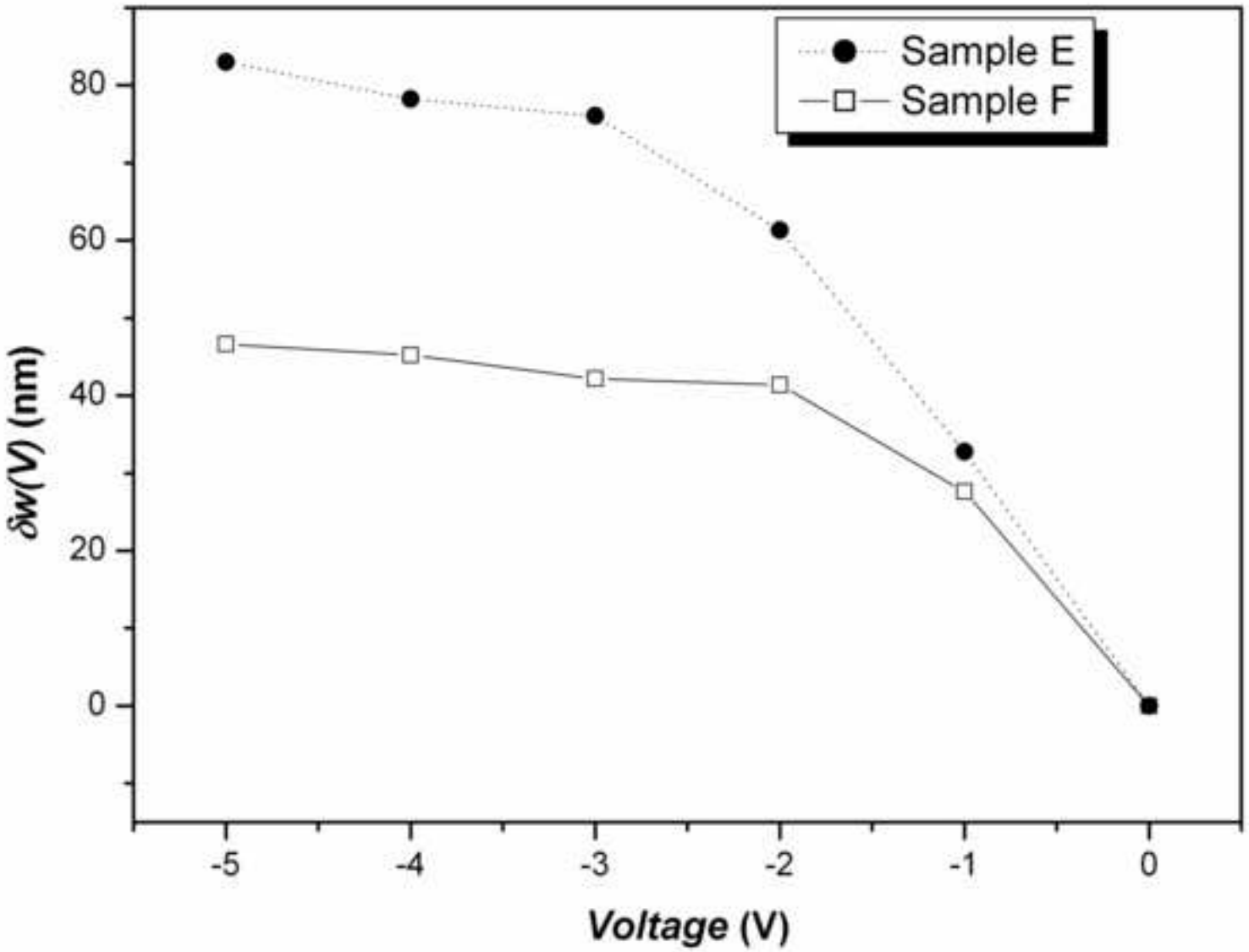

Figure 9

Click here to download high resolution image

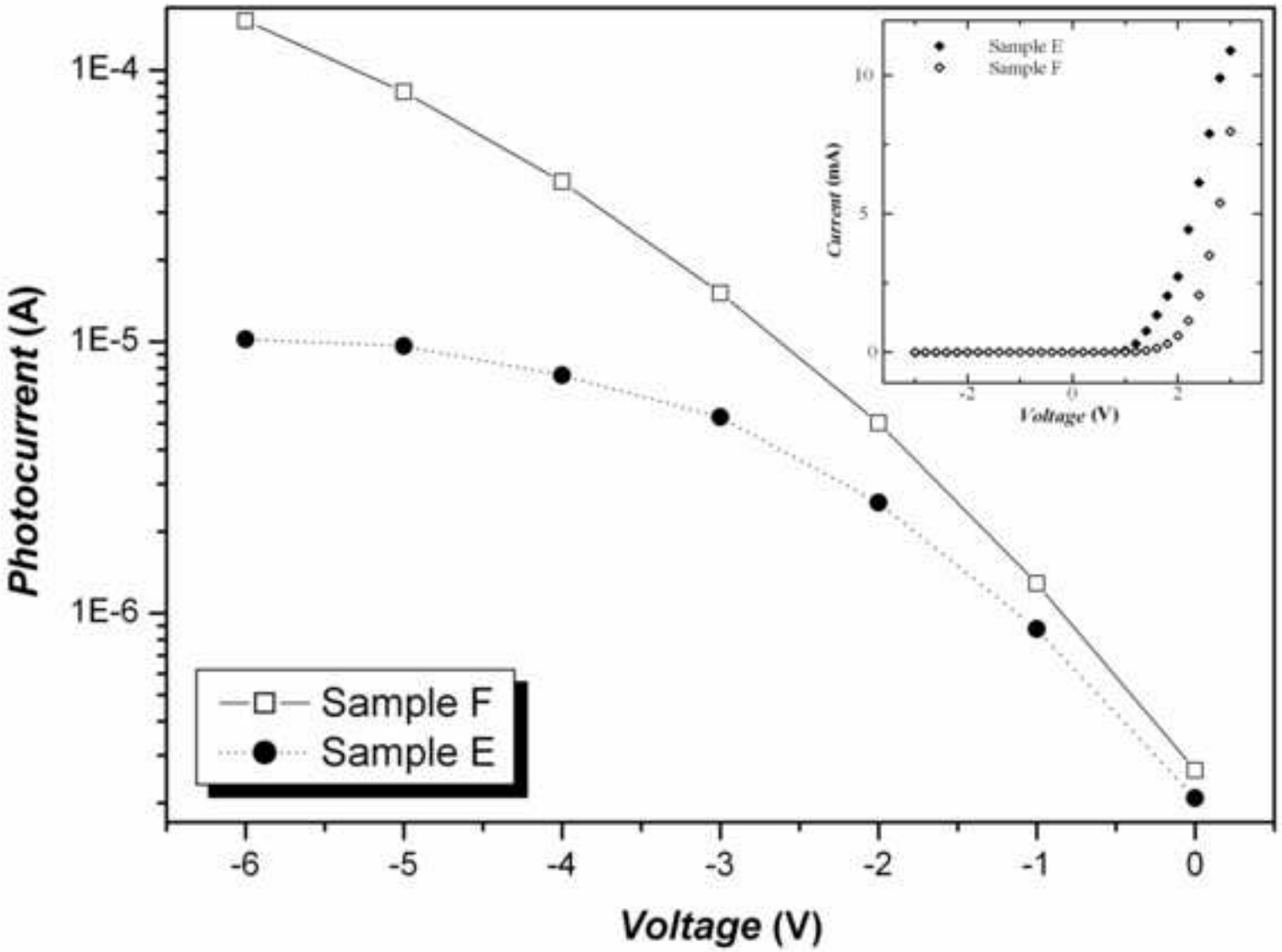

Figure 10

Click here to download high resolution image